

Study on 0^+ states with open charm in unitarized heavy meson chiral approach

P. WANG¹, X.G. WANG²

*Institute of High Energy Physics, CAS, Beijing 100049, P. R. China
Theoretical Physics Center for Science Facilities, CAS, Beijing 100049, P. R. China*

Abstract

We calculate the scattering amplitudes of Goldstone bosons off the pseudoscalar D-mesons in unitarized heavy meson chiral approach. The low energy constants appearing in $\mathcal{O}(p^2)$ chiral Lagrangian are determined by fitting lattice simulations on S -wave scattering lengths. $D_{s0}^*(2317)$ is obtained as a bound state in $(S, I) = (1, 0)$ DK channel. Possible bound states or resonance states in other channels are investigated as well. The quark mass dependence of the mass and binding energy of $D_{s0}^*(2317)$ is also investigated, which indicates predominately DK molecular nature.

1 Introduction

In the last decade, the discovery of many narrow resonances with open charm open a new chapter in hadronic spectroscopy. Especially, the $D_{s0}^*(2317)$ discovered by the BaBar Collaboration [1] and $D_{s1}(2460)$ by the CLEO Collaboration [2] have inspired heated discussions both experimentally and theoretically. Moreover, the Belle Collaboration recently reported a broad 0^+ charmed meson with mass and width being $m_{D_0^{*0}} = 2308 \pm 60 \text{ MeV}$ and $\Gamma_{D_0^{*0}} = 276 \pm 99 \text{ MeV}$, respectively [3]. Meanwhile, the FOCUS Collaboration reported a broad 0^+ charmed meson with mass and width being $m_{D_0^{*0}} = 2407 \pm 56 \text{ MeV}$ and $\Gamma_{D_0^{*0}} = 240 \pm 114 \text{ MeV}$, respectively [4]. Although consistent with each other within the errors, it is still in dispute whether they are the same particle [5].

Possible interpretations of $D_{s0}^*(2317)$ include normal $c\bar{s}$ state [6], four-quark state [7], hadron molecular state [8], etc. To distinguish composite from elementary particles, different methods were proposed such as pole counting [9], scattering length and effective range [10]. As emphasized in a series of paper [11, 12], quark mass dependence of a state can also provide important information on its nature.

Effective field theories (EFTs) have been proven very successful in studying low energy hadron physics [13]. In light meson sector, chiral perturbation theory is an expansion in powers of external momenta and masses of Goldstone bosons [14, 15]. In high energy region or for large quark masses, chiral amplitudes violate unitarity severely. In addition, chiral expansion up to a given finite order does not contain resonance or bound state, which may modify the results of physical variables from perturbation theory significantly. Therefore, unitarized model was introduced to

¹Email address: pwang4@ihep.ac.cn

²Email address: wangxg84@ihep.ac.cn

high energy region, in which lower lying scalar and vector resonances can be dynamically generated. Following the same spirit, heavy meson chiral perturbation theory (HMChPT) was proposed [16–18], and unitarization method was applied to some phenomenological analysis [19–23].

Lattice gauge theory is another powerful tool to study strong interactions. Lattice simulations are usually performed at unphysical quark masses, or equivalently at larger pion masses. Recently, lattice results for the charmed meson-light hadron scattering lengths are given at several chosen values of M_π/F_π [24]. These progresses can be used to make up the lack of experimental data on scattering processes. These lattice data can be used to determine the low energy constants in perturbative scattering amplitudes [25].

$D_{s0}^*(2317)$ as well as other possible charmed particles were investigated with the unitarized heavy meson chiral approach by studying the scattering lengths of charmed mesons and Goldstone bosons in Ref. [12, 23]. The quark mass dependence of the poles has an interesting behavior and provides a good way to understand the structure of the obtained poles. In their calculation, the large N_C approximation and the mass and width of $D_{s0}^*(2317)$ as input are used to determine the low energy constants. In this paper, we use the similar approach to reinvestigate the charmed mesons scattering off light mesons. The difference between our treatment and theirs is that we do not apply the large N_C approximation. This is because in the real world, N_C is 3. Moreover, in the large N_C limit, the mass and width of the particle can be quite different from the real particle [28–30]. Therefore, three additional low energy constants (LECs) h_0 , h_2 and h_4 appear in our case. The parameter h_1 can be determined by the mass difference between D mesons. The parameter h_0 is obtained by the quark mass dependence of D and Ds mesons from the lattice data [27]. The other constants including h_3 and h_5 are determined by fitting the lattice data of the scattering lengths of D and light mesons [24]. To confirm the existence of $D_{s0}^*(2317)$, its mass and width are not used as input. All the states including $D_{s0}^*(2317)$ will be obtained from pole analysis on the scattering amplitudes. As a comparison, the quark mass dependence of $D_{s0}^*(2317)$ is also discussed.

The paper is organized as follows. In sect. 2, we briefly introduce the effective chiral Lagrangian up to next-to-leading order. We calculate the perturbative scattering amplitudes and perform unitarization in sect. 3. The low energy constants are determined by fitting lattice simulations on S -wave scattering lengths in sect. 4. In sect. 5, we present the possible bound states or resonant poles in appropriate channels, and then investigate the quark mass dependence of $D_{s0}^*(2317)$. Finally, We make a brief summary in sect. 6.

2 The effective Lagrangian

The leading order chiral Lagrangian for describing the interaction between the Goldstone boson and the heavy pseudoscalar meson is [16–18]

$$\mathcal{L}^{(1)} = \mathcal{D}_\mu D D^\mu D^\dagger - \overset{\circ}{M}_D^2 D D^\dagger \quad (1)$$

with $D = (D^0, D^+, D_s^+)$. The covariant derivative is

$$\begin{aligned}\mathcal{D}_\mu D^\dagger &= (\partial_\mu + \Gamma_\mu) D^\dagger, \\ \Gamma_\mu &= \frac{1}{2}(u^\dagger \partial_\mu u + u \partial_\mu u^\dagger),\end{aligned}\quad (2)$$

where

$$U = \exp\left(\frac{\sqrt{2}i\phi}{F}\right), \quad u^2 = U, \quad (3)$$

with ϕ containing the Goldstone boson fields,

$$\phi(x) = \begin{pmatrix} \frac{1}{\sqrt{2}}\pi^0 + \frac{1}{\sqrt{6}}\eta & \pi^+ & K^+ \\ \pi^- & -\frac{1}{\sqrt{2}}\pi^0 + \frac{1}{\sqrt{6}}\eta & K^0 \\ K^- & \bar{K}^0 & -\frac{2}{\sqrt{6}}\eta \end{pmatrix}. \quad (4)$$

F is the Goldstone boson decay constant in the chiral limit, which we will identify with the pion decay constant, $F = 92.4\text{MeV}$.

The strong interaction part of NLO chiral Lagrangian reads ³

$$\begin{aligned}\mathcal{L}_{\text{str.}}^{(2)} &= D(-h_0\langle\chi_+\rangle - h_1\chi_+ + h_2\langle u_\mu u^\mu\rangle - h_3u_\mu u^\mu)\bar{D} \\ &+ \mathcal{D}_\mu D(h_4\langle u^\mu u^\nu\rangle - h_5\{u^\mu, u^\nu\} - h_6[u^\mu, u^\nu])\mathcal{D}_\nu\bar{D},\end{aligned}\quad (5)$$

where $\langle\rangle$ stands for the trace of the 3×3 matrices, and

$$\begin{aligned}\chi_+ &= u^\dagger \chi u^\dagger + u \chi u, \\ u_\mu &= iu^\dagger \mathcal{D}_\mu U u^\dagger.\end{aligned}\quad (6)$$

with

$$\chi = 2B \cdot \text{diag}(m_u, m_d, m_s). \quad (7)$$

The term proportional to h_0 leads to a singlet contribution to the D -meson masses which depends linearly on the light quark masses, and is the heavy meson analog of the pion-nucleon sigma term [26]. The h_1 term will contribute to the $SU(3)_V$ -violating mass splitting amongst D mesons. The masses of D and D_s mesons can be expressed as

$$\begin{aligned}M_D^2 &= \overset{\circ}{M}_D^2 + 4h_0B(m_u + m_d + m_s) + 4h_1B\hat{m}, \\ M_{D_s}^2 &= \overset{\circ}{M}_{D_s}^2 + 4h_0B(m_u + m_d + m_s) + 4h_1Bm_s,\end{aligned}\quad (8)$$

from which we can determine

$$h_1 = \frac{M_{D_s}^2 - M_D^2}{4B(m_s - \hat{m})} = \frac{M_{D_s}^2 - M_D^2}{4(M_K^2 - M_\pi^2)} = 0.427, \quad (9)$$

where $\hat{m} = (m_u + m_d)/2$ and the mass relations of Goldstone bosons from leading order chiral expansion,

$$M_\pi^2 = 2B\hat{m}, \quad M_K^2 = B(\hat{m} + m_s), \quad M_\eta^2 = \frac{2}{3}B(\hat{m} + 2m_s), \quad (10)$$

are used. We can simply estimate the value of h_0 to be 0.055 according to the slope of the extrapolation curve from lattice [27].

³The h_1 term is a little different from [23] in order that the term $D\langle\chi_+\rangle\bar{D}$ will completely disappear in large N_C limit [19]. The corresponding coefficients C_1 are also modified (see Tab. 1).

(S, I)	Channel	C_{LO}	C_1	C_{35}	C_0	C_{24}
$(-1, 0)$	$D\bar{K} \rightarrow D\bar{K}$	-1	$3M_K^2$	-1	$-M_K^2$	-1
$(-1, 1)$	$D\bar{K} \rightarrow D\bar{K}$	1	$-3M_K^2$	1	$-M_K^2$	-1
$(0, \frac{1}{2})$	$D\pi \rightarrow D\pi$	-2	$-3M_\pi^2$	1	$-M_\pi^2$	-1
	$D\eta \rightarrow D\eta$	0	$-M_\pi^2$	$\frac{1}{3}$	$-M_\eta^2$	-1
	$D_s\bar{K} \rightarrow D_s\bar{K}$	-1	$-3M_K^2$	1	$-M_K^2$	-1
	$D\eta \rightarrow D\pi$	0	$-3M_\pi^2$	1	0	0
	$D_s\bar{K} \rightarrow D\pi$	$-\frac{\sqrt{6}}{2}$	$-\frac{3\sqrt{6}}{4}(M_K^2 + M_\pi^2)$	$\frac{\sqrt{6}}{2}$	0	0
	$D_s\bar{K} \rightarrow D\eta$	$-\frac{\sqrt{6}}{2}$	$\frac{\sqrt{6}}{4}(5M_K^2 - 3M_\pi^2)$	$-\frac{\sqrt{6}}{6}$	0	0
	$D\pi \rightarrow D\pi$	1	$-3M_\pi^2$	1	$-M_\pi^2$	-1
	$D\pi \rightarrow D\pi$	1	$-3M_\pi^2$	1	$-M_\pi^2$	-1
$(1, 0)$	$DK \rightarrow DK$	-2	$-6M_K^2$	2	$-M_K^2$	-1
	$D_s\eta \rightarrow D_s\eta$	0	$-2(2M_K^2 - M_\pi^2)$	$\frac{4}{3}$	$-M_\eta^2$	-1
	$D_s\eta \rightarrow DK$	$-\sqrt{3}$	$\frac{\sqrt{3}}{2}(3M_\pi^2 - 5M_K^2)$	$\frac{\sqrt{3}}{3}$	0	0
$(1, 1)$	$D_s\pi \rightarrow D_s\pi$	0	0	0	$-M_\pi^2$	-1
	$DK \rightarrow DK$	0	0	0	$-M_K^2$	-1
	$DK \rightarrow D_s\pi$	1	$-\frac{3}{2}(M_K^2 + M_\pi^2)$	1	0	0
$(2, \frac{1}{2})$	$D_sK \rightarrow D_sK$	1	$-3M_K^2$	1	$-M_K^2$	-1

Table 1: The coefficients in the scattering amplitudes. Here, S (I) denotes the total strangeness (isospin) of the two-meson system.

3 Scattering amplitudes and unitarization

The perturbative chiral amplitudes up to NLO can be easily obtained. Besides the terms in Ref. [23] where large N_C suppressed ones are omitted, there are two additional terms (last two terms in Eq. (11)). Although suppressed in large N_C limit, the contributions from h_0 , h_2 and h_4 terms may not be negligible since we are working at $N_C = 3$. On the other hand, complete large N_C analysis in light meson sector shows that poles will move far away from their physical positions as increasing N_C [28–30]. Therefore, in this paper we include the complete tree level amplitude with definite strangeness and isospin up to $\mathcal{O}(p^2)$, which can be written as⁴

$$\begin{aligned}
T(s, t, u) &= T^{(1)}(s, t, u) + T^{(2)}(s, t, u) \\
&= \frac{C_{LO}}{4F^2}(s - u) + \frac{2C_1}{3F^2}h_1 + \frac{2C_{35}}{F^2}H_{35}(s, t, u) \\
&\quad + \frac{4C_0}{F^2}h_0 + \frac{2C_{24}}{F^2}H_{24}(s, t, u), \tag{11}
\end{aligned}$$

⁴Here, we adopt the same convention for the isospin decompositions as Ref. [23].

where the subscripts denote the chiral dimension and the functions H_{35} and H_{24} are expressed as

$$\begin{aligned} H_{35}(s, t, u) &= h_3 p_2 \cdot p_4 + h_5 (p_1 \cdot p_2 p_3 \cdot p_4 + p_1 \cdot p_4 p_2 \cdot p_3) , \\ H_{24}(s, t, u) &= 2h_2 p_2 \cdot p_4 + h_4 (p_1 \cdot p_2 p_3 \cdot p_4 + p_1 \cdot p_4 p_2 \cdot p_3) . \end{aligned} \quad (12)$$

The coefficients in all the amplitudes are given in Tab. 1. We also dropped the h_6 term as in Ref. [23] since it is suppressed by one order due to the commutator structure. The tree level amplitudes can be projected to the S -wave by using

$$V_{ij}^{(S,I)}(s) = \frac{1}{2} \int_{-1}^1 d \cos \theta T_{ij}^{(S,I)}(s, t(s, \cos \theta), u(s, \cos \theta)) , \quad (13)$$

where

$$\begin{aligned} u(s, \cos \theta) &= m_1^2 + m_4^2 - \frac{1}{2s} [s + m_1^2 - m_2^2][s + m_4^2 - m_3^2] \\ &\quad - \frac{1}{2s} \sqrt{\lambda(s, m_1^2, m_2^2) \lambda(s, m_3^2, m_4^2)} \cos \theta , \end{aligned} \quad (14)$$

with

$$\lambda(s, m_i^2, m_j^2) = [s - (m_i + m_j)^2][s - (m_i - m_j)^2] . \quad (15)$$

In [31–33], a general method was proposed to construct scattering amplitudes satisfying unitarity, i.e.

$$T(s) = V(s)[1 - G(s) \cdot V(s)]^{-1} , \quad (16)$$

where V is a matrix whose elements are given by Eq. (13) and G is a diagonal matrix with the element being a two-meson integral

$$G_{ii}(s) = i \int \frac{d^4 q}{(2\pi)^4} \frac{1}{q^2 - m_1^2 + i\epsilon} \frac{1}{(p_1 + p_2 - q)^2 - m_2^2 + i\epsilon} , \quad (17)$$

with m_1 and m_2 the masses of the particles appearing in the loop. The analytic expression of $G_{ii}(s)$ can be expressed by [33]

$$\begin{aligned} G_{ii} &= \frac{1}{16\pi^2} \left\{ a(\mu) + \log \frac{m_1^2}{\mu^2} + \frac{\Delta - s}{2s} \log \frac{m_1^2}{m_2^2} \right. \\ &\quad \left. + \frac{\sigma}{2s} [\log(s - \Delta + \sigma) + \log(s + \Delta + \sigma) - \log(-s + \Delta + \sigma) - \log(-s - \Delta + \sigma)] \right\} , \end{aligned} \quad (18)$$

where

$$\sigma = [-(s - (m_1 + m_2)^2)(s - (m_1 - m_2)^2)]^{1/2} , \quad \Delta = m_1^2 - m_2^2 . \quad (19)$$

$a(\mu)$ is the subtraction constant with μ the regularization scale. In the numerical calculation, we tried three possible values of $a(m_D)$ estimated in Ref. [21]. The S -wave scattering length is defined as

$$a_0 = -\frac{1}{8\pi(M_1 + M_2)} T_{\text{thr}} , \quad (20)$$

$a(m_D)$	-0.373	-0.630	-0.864
h_2	-0.216 ± 0.178	-0.195 ± 0.197	-0.127 ± 0.209
h_3	0.393 ± 0.698	0.510 ± 1.083	-0.015 ± 1.754
h_4	0.061 ± 0.046	0.056 ± 0.050	0.038 ± 0.053
h_5	-0.001 ± 0.091	0.032 ± 0.141	0.172 ± 0.229
$\chi^2_{d.o.f}$	$43.4/12 = 3.6$	$43.6/12 = 3.6$	$42.1/12 = 3.5$

Table 2: The fit results on LECs corresponding to different values of $a(m_D)$ taken from Ref. [21]. h_2 and h_3 are dimensionless, while h_4 and h_5 are in unit of GeV^{-2} .

with M_1 and M_2 denoting the masses of the scattered heavy and light mesons, respectively. T_{thr} is the unitarized amplitude at threshold, $s = (M_1 + M_2)^2$. The physical masses for all mesons are taken from PDG [34], i.e., $M_\pi = 138 \text{ MeV}$, $M_K = 496 \text{ MeV}$, $M_\eta = 548 \text{ MeV}$, $M_D = 1867 \text{ MeV}$, and $M_{D_s} = 1968 \text{ MeV}$.

4 Determination of LECs

There are no experimental data for the scattering of Goldstone bosons off D -mesons available. However, the low energy constants entering into NLO Lagrangian $\mathcal{L}_{\text{str.}}^{(2)}$ can be determined by fitting the recent lattice simulations on S -wave scattering lengths [24]. The lattice spacing is $b = 0.12\text{fm}$. The s quark mass is 80MeV , which is consistent with its physical mass, and four ensembles are chosen with $M_\pi = 0.1842, 0.2238, 0.3113, 0.3752$ in lattice unit, or equivalently $M_\pi = 0.2925, 0.3554, 0.4943, 0.5958$ in unit of GeV .⁵

From Eq. (8), the pion mass dependence of D mesons up to $\mathcal{O}(M_\pi^2)$ can be expressed as

$$\begin{aligned}
M_D(M_\pi) &= M_D|_{phy} + \frac{2h_0 + h_1}{M_D|_{phy}}(M_\pi^2 - M_\pi^2|_{phy}), \\
M_{D_s}(M_\pi) &= M_{D_s}|_{phy} + \frac{2h_0}{M_{D_s}|_{phy}}(M_\pi^2 - M_\pi^2|_{phy}),
\end{aligned} \tag{21}$$

and from Eq. (10) we can get

$$M_K(M_\pi) = \dot{M}_K + \frac{M_\pi^2}{4\dot{M}_K}, \quad M_\eta(M_\pi) = \dot{M}_\eta + \frac{M_\pi^2}{6\dot{M}_\eta}, \tag{22}$$

where $\dot{M}_K = 486\text{MeV}$ and $\dot{M}_\eta = 542\text{MeV}$ are the masses of kaon and η in the chiral limit, respectively. Thus, the scattering length defined by Eq. (20) is a function of M_π .

Although $(S, I) = (1, 1)$ is in fact a couple channel case, we use single channel

⁵These lattice data were misused in [23].

(S, I)	Channel	LO	NLO	UChPT	CUChPT	Lattice [24]
$(-1, 0)$	$D\bar{K} \rightarrow D\bar{K}$	0.36	0.54	-1.24		-0.23(4)
$(-1, 1)$	$D\bar{K} \rightarrow D\bar{K}$	-0.36	-0.49	-0.21		
$(0, \frac{1}{2})$	$D\pi \rightarrow D\pi$	0.24	0.23	0.41	0.39	
	$D\eta \rightarrow D\eta$	0	-0.06	-0.05	$-1.48 + i0.04$	
	$D_s\bar{K} \rightarrow D_s\bar{K}$	0.36	0.23	0.58	$-0.67 + i0.10$	-0.16(4)
$(0, \frac{3}{2})$	$D\pi \rightarrow D\pi$	-0.12	-0.13	-0.10		
$(1, 0)$	$DK \rightarrow DK$	0.72	0.46	-1.99	-0.73	
	$D_s\eta \rightarrow D_s\eta$	0	-0.16	-0.11	$-0.35 + i0.05$	
$(1, 1)$	$D_s\pi \rightarrow D_s\pi$	0	0.003	0.003	0.01	0.00(1)
	$DK \rightarrow DK$	0	0.02	0.03	$-0.52 + i0.22$	
$(2, \frac{1}{2})$	$D_sK \rightarrow D_sK$	-0.36	-0.51	-0.22		-0.31(2)

Table 3: The S-wave scattering lengths from calculations at LO and NLO (units are fm). The results using unitarized amplitudes are also given in the two columns denoted by UChPT and CUChPT, representing one-channel and coupled-channel unitarized chiral perturbation theory, respectively.

unitarization in our fit procedure for all of the four channels, since so far lattice data only exist without channel coupling. The obtained LECs in three cases are shown in Tab. 2, corresponding to different values of $a(m_D)$ which were estimated by comparing the dispersion relation method with the cut-off method [21]. $a(m_D)$ chosen to be -0.373 , -0.630 and -0.864 correspond to the resultant cut-off momentum q_{max} at 0.6, 0.8 and 1.0 GeV, respectively. In Fig. 1, we plot the fitted results of the scattering lengths versus pion mass with $a(m_D) = -0.864$ since all the three choices of $a(m_D)$ give similar curves. One can see that lattice data can be fitted very well except the $(S, I) = (2, 1/2)$ channel. The scattering lengths of $(S, I) = (0, 3/2)$ and $(S, I) = (1, 1)$ channels are sensitive to pion mass which can be understood from Tab. 1. The scattering lengths of $(S, I) = (-1, 1)$ and $(S, I) = (2, 1/2)$ channels change little with the increasing pion mass. The calculation with the heavy meson chiral perturbation theory is not completely consistent with the lattice data of $(S, I) = (2, 1/2)$ channel which deserves further investigation. Without the large N_C suppression terms, the scattering length of $(S, I) = (1, 1)$ channel remains zero with the increasing pion mass.⁶ The inclusion of these terms improves the fit of lattice data.

⁶In Ref. [23], with their notation, the coefficient $C_1 = 2M_\pi^2$ makes the scattering lengths of $(S, I) = (1, 1)$ channel be always negative and decrease with increasing pion mass.

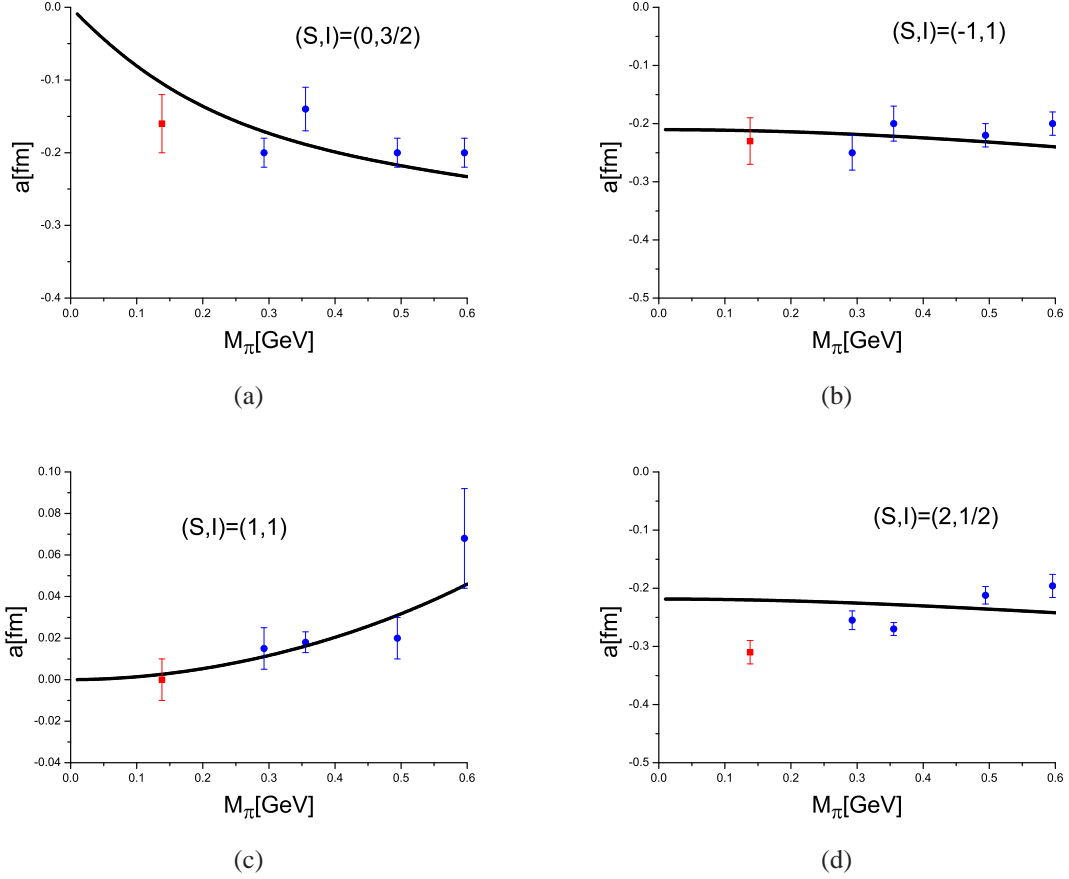


Figure 1: The fitted results on scattering lengths. The squares(red) denote chiral extrapolation results given by [24], which are *not* included in our fit.

5 Pole analysis

5.1 Pole positions in appropriate channels

Under the present convention, the relationship between S matrix and T matrix is given by

$$S_{ij} = \delta_{ij} - \frac{2i}{8\pi} \frac{\sqrt{k_i k_j}}{\sqrt{s}} T_{ij}(s), \quad (23)$$

with k_i the i -th channel momentum. In general, for a system with N open channels, we have in total 2^N Riemann sheets, which can be enumerated as $L(\sigma_1, \sigma_2, \dots, \sigma_N)$ where σ_i stands for the sign of $\text{Im}k_i$ [35]. Taking 2-channel case for example, we enumerate the 4 sheets in the following way,

$$\begin{aligned} \text{sheet I :} & \quad \text{Im}k_1 > 0, \text{Im}k_2 > 0, L(++) , \\ \text{sheet II :} & \quad \text{Im}k_1 < 0, \text{Im}k_2 > 0, L(-+) , \\ \text{sheet III :} & \quad \text{Im}k_1 < 0, \text{Im}k_2 < 0, L(--) , \\ \text{sheet IV :} & \quad \text{Im}k_1 > 0, \text{Im}k_2 < 0, L(+-) . \end{aligned} \quad (24)$$

(S,I)	Channel	Thr	RS	Fit I	Fit II	Fit III
(-1,0)	$D\bar{K} \rightarrow D\bar{K}$	2363	I			2340
			II	$2315 - i70$	2194	
$(0, \frac{1}{2})$	$D\pi \rightarrow D\pi$	2005	II	$2146 - i124$	$2122 - i93$	$2104 - i75$
	$D\eta \rightarrow D\eta$	2415	III	$2478 - i23$	$2434 - i19$	$2376 - i1$
	$D_s\bar{K} \rightarrow D_s\bar{K}$	2464				
(1,0)	$DK \rightarrow DK$	2363	I	2356	2327	2295
	$D_s\eta \rightarrow D_s\eta$	2516				
(1,1)	$D_s\pi \rightarrow D_s\pi$	2106	II	$2433 - i26$	$2372 - i39$	$2318 - i37$
	$DK \rightarrow DK$	2363				

Table 4: Pole positions on \sqrt{s} plane in unit of MeV. Thr and RS denote channel threshold and Riemann Sheet, respectively.

The analytic continuation of S matrix to different sheets can be obtained

$$S^{II} = \begin{pmatrix} \frac{1}{S_{11}} & \frac{iS_{12}}{S_{11}} \\ \frac{iS_{12}}{S_{11}} & \frac{\det S}{S_{11}} \end{pmatrix}, \quad S^{III} = \begin{pmatrix} \frac{S_{22}}{\det S} & \frac{-S_{12}}{\det S} \\ \frac{-S_{12}}{\det S} & \frac{S_{11}}{\det S} \end{pmatrix}, \quad S^{IV} = \begin{pmatrix} \frac{\det S}{S_{22}} & \frac{-iS_{12}}{S_{22}} \\ \frac{-iS_{12}}{S_{22}} & \frac{1}{S_{22}} \end{pmatrix}, \quad (25)$$

from which we can see that the poles on sheet-II and sheet-III correspond to zeroes of $S_{11}(s)$ and $\det S = S_{11}S_{22} - S_{12}S_{21}$, respectively.

Corresponding to each set of parameters given by Tab. 2, we list the pole positions found in appropriate channels in Tab. 4, from which one can see all the three parameter sets give similar results except for the $(S, I) = (-1, 0)$ channel. For the mass and width of each pole in other channels, taking into account the uncertainty of $a(\mu)$ in Tab. 4, we will take $(M_{max} + M_{min})/2$ among the three fits as the central value and $(M_{max} - M_{min})/2$ as the error.

In $(S, I) = (-1, 0)$ channel, the pole structure is unstable. Pole positions are dependent on the strength of interactions, which is governed by LECs. In fit I, we find a “resonance”, whose position is similar to [23]. However, it has no physical correspondence since a particle with mass below the lowest hadron-hadron threshold can not possess finite width by strong decay. In fit II, there is a virtual state, which is located on the real axis below $D\bar{K}$ threshold on the second Riemann sheet. The bound state pole predicted by fit III is in agreement with [20]. Further experiments on this channel will determine which parameter set is more reasonable.

In $(S, I) = (0, 1/2)$ channel, we perform 3-channel unitarization. We find a broad second sheet pole at $(2125 \pm 21 - i100 \pm 25)\text{MeV}$ and a narrow third sheet pole at $(2427 \pm 51 - i12 \pm 11)\text{MeV}$, respectively. Although still deviate from the experimental data [3, 4], our results are in agreement with [20, 21]. Ref. [22] gave some arguments to explain why resonances predicted theoretically have not been observed by experiment. In addition to production rate, finding a new state exper-

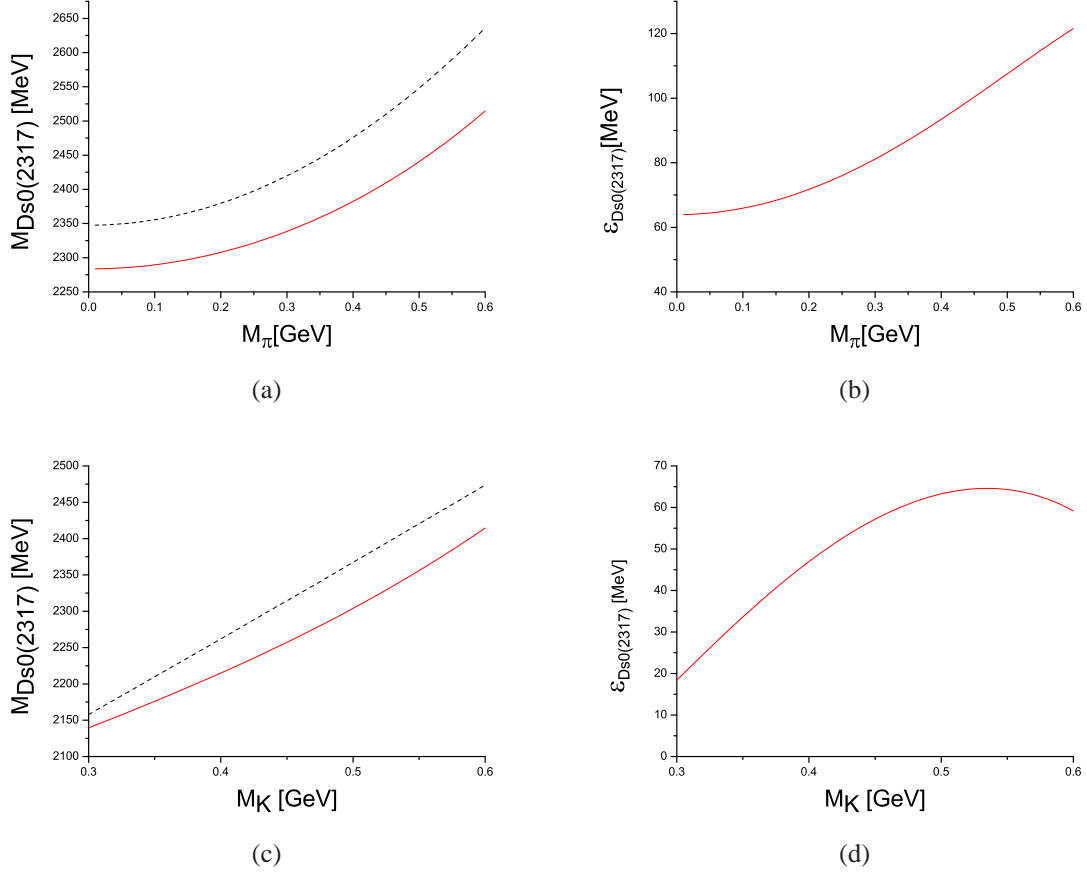


Figure 2: a) Pion mass dependence of the mass of $D_{s0}^*(2317)$ (solid) and DK threshold(dashed); b) Pion mass dependence of binding energy; c) Kaon mass dependence of the mass of $D_{s0}^*(2317)$ (solid) and DK threshold(dashed); d) Kaon mass dependence of binding energy.

imentally also depends on data measurements and analysis, which are affected by many factors, such as data statistics, the background, etc.

A bound state pole of $D_{s0}^*(2317)$ in $(S, I) = (1, 0)$ channel is obtained. In Ref. [12, 23], the bound state of $D_{s0}^*(2317)$ is assumed and its mass is used as an input to determine the LECs. Here, $D_{s0}^*(2317)$ is really obtained from the analysis of the poles. The mass of $D_{s0}^*(2317)$ in our analysis is $m = 2326 \pm 30 \text{ MeV}$, which is in agreement with [21].

In $(S, I) = (1, 1)$ channel, only N_C suppressed terms contribute to the elastic scattering amplitudes, as can be seen from Tab. 1. The nearest resonance pole to the physical region is located on sheet II at $(2376 \pm 58 - i33 \pm 7) \text{ MeV}$. The position of this state is different from that obtained in Ref. [21] where a resonance on sheet III with smaller mass and larger width exists.

5.2 Quark mass dependence

The mass and width of the states are obtained in the last subsection. But we did not get the information about the nature of the states. There are some methods to determine the structure of a particle, as mentioned in the introduction. In Ref. [12, 23], the authors studied the structure by investigating the quark mass dependence of the states. This method provides a direct and clear picture for the composition of a particle. We now make the similar analysis as in Ref. [23]. We first fix s quark mass and vary the light quark masses. In Fig. 2a and 2b, we show the mass of $D_{s0}^*(2317)$, as well as the binding energy as a function of the pion mass. Both the mass and binding energy increase with the increasing pion mass. A pure $c\bar{s}$ state has no constituent light quarks. Its light quark mass dependence only comes from sea quark contributions, which should be very weak as the case of $D_s(1968)$ shown in lattice simulations [27]. The sensitive dependence of light quark mass shows that $D_{s0}^*(2317)$ may probably be a DK molecular or tetraquark state where the constituent light quark exists.

Some general discussions on the importance of kaon mass dependence have been made in Ref. [12]. The mass of kaon-hadron molecular state is given by

$$M = M_K + M_h - \epsilon, \quad (26)$$

where M_h is the mass of the other hadron and ϵ is the binding energy. The leading kaon mass dependence of such a bound state is linear, and the slop is unity.

To study the kaon mass dependence of $D_{s0}^*(2317)$, we fix the pion mass at its physical value, and express all results in terms of M_K . From Eq. (8) and (10), we can obtain

$$\begin{aligned} M_D(M_K) &= M_D|_{phy} + \frac{2h_0}{M_D|_{phy}}(M_K^2 - M_K^2|_{phy}), \\ M_{Ds}(M_K) &= M_{Ds}|_{phy} + \frac{2(h_0 + h_1)}{M_{Ds}|_{phy}}(M_K^2 - M_K^2|_{phy}), \end{aligned} \quad (27)$$

and $M_\eta(M_K) = \sqrt{\frac{4}{3}M_K^2 - \frac{1}{3}M_\pi^2|_{phy}}$.

Fig. 2c and 2d show the mass and binding energy of $D_{s0}^*(2317)$ as a function of kaon mass. The K -meson mass dependence of $D_{s0}^*(2317)$ is almost linear which is really in good agreement with the DK molecular expectation. These results are comparable with Ref. [12].

6 Summary

In this paper, we calculate the complete scattering amplitudes of Goldstone bosons off the pseudoscalar D-mesons using unitarized heavy meson chiral approach. Two low energy constants h_0 and h_1 are determined by the mass splitting among D mesons and pion mass dependence of D and D_s . The other four LECs are determined by fitting lattice simulations on S -wave scattering lengths. The large

N_C suppressed terms improve the fit. Three sets of parameters are obtained according to different choices of the subtraction constant $a(m_D)$. All the three sets of parameters give similar scattering lengths which are close to the lattice results.

$D_{s0}^*(2317)$ is obtained as a bound state in $(S, I) = (1, 0)$ channel, with the mass being $m = 2326 \pm 30 \text{ MeV}$. The strong pion mass dependence of its mass and binding energy disfavors conventional $c\bar{s}$ content. The approximately linear kaon mass dependence reveals it is predominately a DK molecular state. In $(S, I) = (0, 1/2)$ channel, a broad pole structure is found at $(2125 \pm 21 - i100 \pm 25) \text{ MeV}$ on the second Riemann sheet, and a narrow pole is at $(2427 \pm 51 - i12 \pm 11) \text{ MeV}$ on the third Riemann sheet. A resonance pole also exists on the second Riemann sheet with mass and width $2376 \pm 58 \text{ MeV}$ and $33 \pm 7 \text{ MeV}$ in $(S, I) = (1, 1)$ channel. The position of the pole in the $(S, I) = (-1, 0)$ channel depends on the parameter sets. Further experiments or lattice simulation can determine which parameter set is more reasonable.

Acknowledgement: We would like to thank L.M. Liu, H.W. Lin and H.Q. Zheng for helpful communications.

References

- [1] BaBar Collaboration (B. Aubert *et al.*), Phys. Rev. Lett. **90** (2003) 242001.
- [2] CLEO Collaboration (D. Besson *et al.*), Phys. Rev. D **68** (2003) 032002.
- [3] Belle Collaboration (K. Abe *et al.*), Phys. Rev. D **69** (2004) 112002.
- [4] FOCUS Collaboration (J.M. Link *et al.*), Phys. Lett. B **586** (2004) 11.
- [5] M.E. Bracco *et al.*, Phys. Lett. **B624**(2005)217.
- [6] W.A. Bardeen, E.J. Eichten, C.T. Hill, Phys. Rev. D **68** (2003) 054024;
Y.B Dai, C.S. Huang, C. Liu, S.L. Zhu, Phys. Rev. D **68** (2003) 114011.
- [7] H.Y. Cheng, W.S. Hou, Phys. Lett. B **566** (2003) 193;
Y.Q. Chen, X.Q. Li, Phys. Rev. Lett. **93** (2004) 232001.
- [8] T. Barnes, F.E. Close, H.J. Lipkin, Phys. Rev. D **68** (2003) 054006;
E.E. Kolomeitsev, M.F.M. Lutz, Phys. Lett. B **582** (2004) 39.
- [9] D. Morgan, Nucl. Phys. A **543** (1992) 632.
- [10] S. Weinberg, Phys. Rev. **131** (1963) 440; V. Baru *et al.*, Phys. Lett. B **586** (2004) 53.
- [11] C. Hanhart, J.R. Pelaez, G. Rios, Phys. Rev. Lett. **100** (2008) 152001.
- [12] M. Cleven, F.-K. Guo, C. Hanhart, U.-G. Meißner, Eur. Phys. J. A **47** (2011) 19.

- [13] S. Weinberg, *Physica A* **96** (1979) 327.
- [14] J. Gasser, H. Leutwyler, *Ann. Phys. (NY)* **158** (1984) 142.
- [15] J. Gasser, H. Leutwyler, *Nucl. Phys. B* **250** (1985) 465.
- [16] G. Burdman and J. F. Donoghue, *Phys. Lett. B* **280**, 287 (1992).
- [17] M. B. Wise, *Phys. Rev. D* **45**, 2188 (1992).
- [18] T. M. Yan *et al.*, *Phys. Rev. D* **46**, 1148 (1992) [Erratum-ibid. *D* **55**, 5851 (1997)].
- [19] M.F.M. Lutz, M. Soyeur, *Nucl. Phys. A* **813** (2008) 14.
- [20] J. Hofmann, M.F.M. Lutz, *Nucl. Phys. A* **733** (2004) 142.
- [21] F.-K. Guo *et al.*, *Phys. Lett. B* **641** (2006) 278.
- [22] F.-K. Guo *et al.*, *Phys. Lett. B* **647** (2007) 133.
- [23] F.-K. Guo, C. Hanhart, U.-G. Meißner, *Eur. Phys. J. A* **40** (2009) 171.
- [24] L. Liu, H. W. Lin and K. Orginos, *PoS LATTICE2008* (2008) 112.
- [25] Y.R. Liu, S.L. Zhu, *Phys. Rev. D* **79** (2009) 094026.
- [26] E.E. Jenkins, *Nucl. Phys. B* **412** (1994) 181.
- [27] E. Follana, *et al.*, *Phys. Rev. Lett.* **100** (2008) 062002.
- [28] J. R. Pelaez, *Phys. Rev. Lett.* **92** (2004) 102001; J. R. Pelaez and G. Rios, *Phys. Rev. Lett.* **97** (2006) 242002.
- [29] Z. H. Guo, J. A. Oller, *Phys. Rev. D* **84** (2011) 034005 .
- [30] L.Y. Dai, X.G. Wang, H.Q. Zheng, arXiv:1108.1451 [hep-ph].
- [31] J. A. Oller and U.-G. Meißner, *Phys. Lett. B* **500**, 263 (2001).
- [32] J. A. Oller, E. Oset and A. Ramos, *Prog. Part. Nucl. Phys.* **45** (2000) 157.
- [33] J. A. Oller and E. Oset, *Phys. Rev. D* **60**, 074023 (1999).
- [34] C. Amsler *et al.* [Particle Data Group], *Phys. Lett. B* **667**, 1 (2008).
- [35] A.M. Badalyan, L.P. Kok, M.I. Polikarpov, Yu.A. Simonov, *Phys. Rep.* **82** (1982) 31.